




**Anisotropic magnetotransport in LaAlO<sub>3</sub>/SrTiO<sub>3</sub> nanostructures**Mithun S. Prasad *Institut für Physik, Martin-Luther-Universität Halle-Wittenberg, Von-Danckelmann-Platz 3, 06120 Halle, Germany*Georg Schmidt \**Institut für Physik, Martin-Luther-Universität Halle-Wittenberg, Von-Danckelmann-Platz 3, 06120 Halle, Germany  
and Interdisziplinäres Zentrum für Materialwissenschaften,  
Martin-Luther-Universität Halle-Wittenberg, Heinrich-Damerow-Strasse 4, 06120 Halle, Germany* (Received 12 February 2021; revised 27 July 2021; accepted 27 July 2021; published 20 August 2021)

A number of recent studies indicate that the charge conduction of the LaAlO<sub>3</sub>/SrTiO<sub>3</sub> interface at low temperature is confined to filaments which are linked to structural domain walls in SrTiO<sub>3</sub> with drastic consequences, for example, for the temperature dependence of local transport properties. We demonstrate that as a consequence of these current carrying filaments, on the nano-scale the magnetotransport properties of the interface are highly anisotropic. Our magnetoresistance measurements reveal that the magnetoresistance in different nanostructures (< 500 nm) is random in magnitude and sign. Warming up nanostructures above the structural phase transition temperature (105 K) results in a significant change in magnetoresistance. Even a sign change of the magnetoresistance is possible. The results suggest that domain walls that are differently oriented with respect to the surface exhibit different respective magnetoresistances and the total magnetoresistance is a result of a random domain wall pattern formed during the structural phase transition in SrTiO<sub>3</sub> at cooldown.

DOI: [10.1103/PhysRevB.104.054115](https://doi.org/10.1103/PhysRevB.104.054115)**I. INTRODUCTION**

Interfaces between complex oxides shows great potential for future electronics [1]. Since the discovery of the high-mobility electron gas at the interface of LaAlO<sub>3</sub> (LAO) and SrTiO<sub>3</sub> (STO) in 2004 [2], a lot of studies have been conducted. Those studies revealed more interesting properties of the interface such as two-dimensional superconductivity, induced ferromagnetism, gate tunability, highly efficient spin-charge conversion, etc. [3–6]. The enhanced room temperature mobility of LAO/STO nanowires [7] holds great promise towards its room temperature application. A study conducted by Dubroka *et al.* [8] showed that the confinement region of the electron gas extends into the STO substrate. Resistance anomalies at ~80 and ~160 K were previously reported in structures grown at low oxygen pressure. The origin of the anomaly is often linked to structural phase transitions in STO [9–12], but alternative explanations have been discussed [8]. In 2017 Minhas *et al.* [13] showed that the resistance anomaly can also be observed in material grown at high oxygen pressure when a lateral confinement in a nanostructure exists.

In 2013 scanning superconducting quantum interference device microscopy studies [14] indicated that the interface exhibits channeled current flow at low temperatures. These current-carrying channels are linked to structural domain walls in the STO substrate that appear below a structural phase transition from cubic to tetragonal at a temperature of 105 K ( $T_{PT}$ ) [15]. The distribution of these channels changes every time the interface is warmed above this transition

temperature [15]. Kalisky *et al.* [14] also observed that the redistribution of the channels is completely random. Further studies also confirmed the presence of conducting domain walls [16–18]. These conducting domain walls are aligned along the crystallographic directions [100], [010], [110], and [1 $\bar{1}$ 0]. Furthermore, Harsan Ma *et al.* [18] observed indications of insulating areas in the vicinity of the conducting domain walls. In confined systems, however, the domain walls can start to massively influence the transport properties. In 2017 Goble *et al.* demonstrated that the resistivity perpendicular to a domain wall is higher [12] than along the domain wall.

Almost at the same time an even more drastic effect on transport in LAO/STO nanostructures was demonstrated [13]. A temperature anomaly in the resistance of LAO/STO nanostructures indicates that transport happens only in conducting domain walls, while the surrounding area is completely insulating. More evidence for domain wall conduction was presented only recently by Krantz and Chandrasekhar [19], who found a Hall-effect-like transverse resistance at zero field that can be explained by asymmetrically distributed domain walls that lead to the appearance of transverse voltages upon current flow.

It is plausible that transport effects should exist that are dominated by the domain wall conductance and cannot be explained by the mainstream theory on LAO/STO interface conductivity. These effects would mainly appear in LAO/STO nanostructures because for transport phenomena in large-area LAO/STO the existing complex multiband models are clearly able to explain the observations based on a quasi-two-dimensional (quasi-2D) conducting interface. Based on a process for the fabrication of LAO/STO nanostructures [20],

\*georg.schmidt@physik.uni-halle.de

we have designed a number of experiments that should clearly reveal the interplay of domain wall conductivity, transport, and magnetotransport properties on the nanoscale. In LAO/STO we distinguish two types of domain walls. One type (type 1) is oriented perpendicular to the surface and along the  $[110]$  and  $[1\bar{1}0]$  crystalline directions in the substrate plane. The other type (type 2) is oriented along the  $[100]$  and  $[010]$  crystalline directions in the plane but is tilted with respect to the surface. As a consequence not only the resistivity but also other characteristics of the two types of domain walls may be different. A magnetic field nominally perpendicular to the 2D electron gas would be in the plane of type 1 domain walls and tilted with respect to type 2 domain walls. This different orientation is crucial because in-plane and (partly) perpendicular magnetic fields typically cause magnetoresistance that can be different in magnitude and/or sign, respectively. In addition, it should be noted that due to the different possible in-plane orientations of the different domain walls a current path through a structure can strongly vary in length and resistance depending on the respective contributing domain walls.

The consequences can be checked by the following investigations. (1) Because of the different domain wall types we expect a random distribution of resistance values at low temperature for nominally identical nanostructures. Warming up through  $T_{PT}$  and cooling down again should result in a different configuration and different resistance values for the same structure. (2) Because of the different types of domain walls and their possible alignment within the crystal lattice it may be possible that this randomness will still show some systematics with respect to the crystalline orientation of the nanostructures. (3) Magnetoresistance measurements in a perpendicular magnetic field on nanostructures with a low number of domain walls should yield a result different from large-area LAO/STO and also strongly vary in magnitude and even sign because with respect to the domain walls the magnetic field is either in plane or tilted but never perpendicular. Also these results should be modified by warm-up and cooling

We have designed a set of experiments in which a particular nanostructure design allows us to precisely verify or nullify these assumptions.

## II. FABRICATION

The fabrication of the samples starts with the deposition of a six unit cell layer of LAO on  $\text{TiO}_2$ -terminated STO (001) using pulsed laser deposition in an oxygen atmosphere with  $p_{\text{O}_2}$  of  $10^{-3}$  mbar at  $850^\circ\text{C}$ . Laser fluence and pulse frequency are kept at  $2\text{ J/cm}^2$  and  $2\text{ Hz}$ , respectively. Reflection high-energy electron diffraction is used to monitor the layer thickness with unit cell resolution during the growth. After deposition the sample is slowly cooled down to room temperature while the oxygen pressure is maintained. For nanopatterning we use the process originally published in [20], which uses reactive ion etching with  $\text{BCl}_3$ . With this process we are able to fabricate high-quality nanostructures with lateral dimension down to  $100\text{ nm}$ . The resulting patterned structures are stable at ambient conditions. The samples are bonded, and electrical transport measurements are carried out in a  $^4\text{He}$  bath cryostat

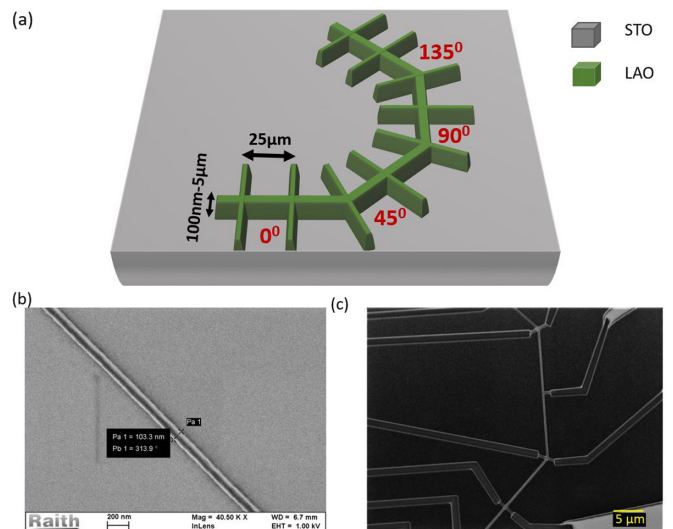


FIG. 1. (a) Sample geometry used for the measurements. The current-carrying path is divided into four equally long sections that are aligned at angles of  $0^\circ$ ,  $45^\circ$ ,  $90^\circ$ , and  $135^\circ$  with respect to the substrate edge. (b) Scanning electron microscope (SEM) image of  $100\text{ nm}$  structures ( $135^\circ$ ) and (c) optical microscope image of part of the  $500\text{ nm}$  wide structure.

with a variable temperature insert equipped with a superconducting magnet that allows a maximum magnetic field of  $10\text{ T}$ .

We used the sample geometry as shown in Fig. 1(a) for the experiments. This geometry was inspired by Hupfauer *et al.* [21], who used a similar structure, but for a different purpose. We have a continuous Hall bar that consists of four connected segments, each with six voltage probes for measurement of longitudinal or transversal resistance. The segments are aligned at  $0^\circ$ ,  $45^\circ$ ,  $90^\circ$ , and  $135^\circ$  with respect to the sample edge, which corresponds to a major crystalline axis ( $100$  or  $010$ ). The samples are cooled down at a rate of approximately  $5\text{ K/min}$ , and warm-up is done at a rate of approximately  $2.5\text{ K/min}$  whenever required. The resistance is always measured in a four-probe geometry. Voltages are measured using custom-made zero-drift voltage amplifiers and an Agilent 34420A 7.5 Digit nanovoltmeter. Current is measured by measuring the voltage over a series resistor of  $1\text{ M}\Omega$ . We apply a DC voltage of  $100\text{ mV}$  across the sample and the series resistor. Because of the design, we are able to measure the resistance of three nanostructures oriented at different respective angles simultaneously keeping all other parameters constant, thus providing higher reproducibility and better comparability of the results. Also, for better understanding and comparison, we have included results from two nominally identical samples labeled sample 1 and sample 2.

## III. MEASUREMENT

As a first test we investigate the temperature dependence of the resistance for four nanostructures of different respective crystalline orientations using the Hall bar geometry from Fig. 1(a) to carry out the resistance measurements. Figure 2(a) shows the temperature dependence (results from sample 1).

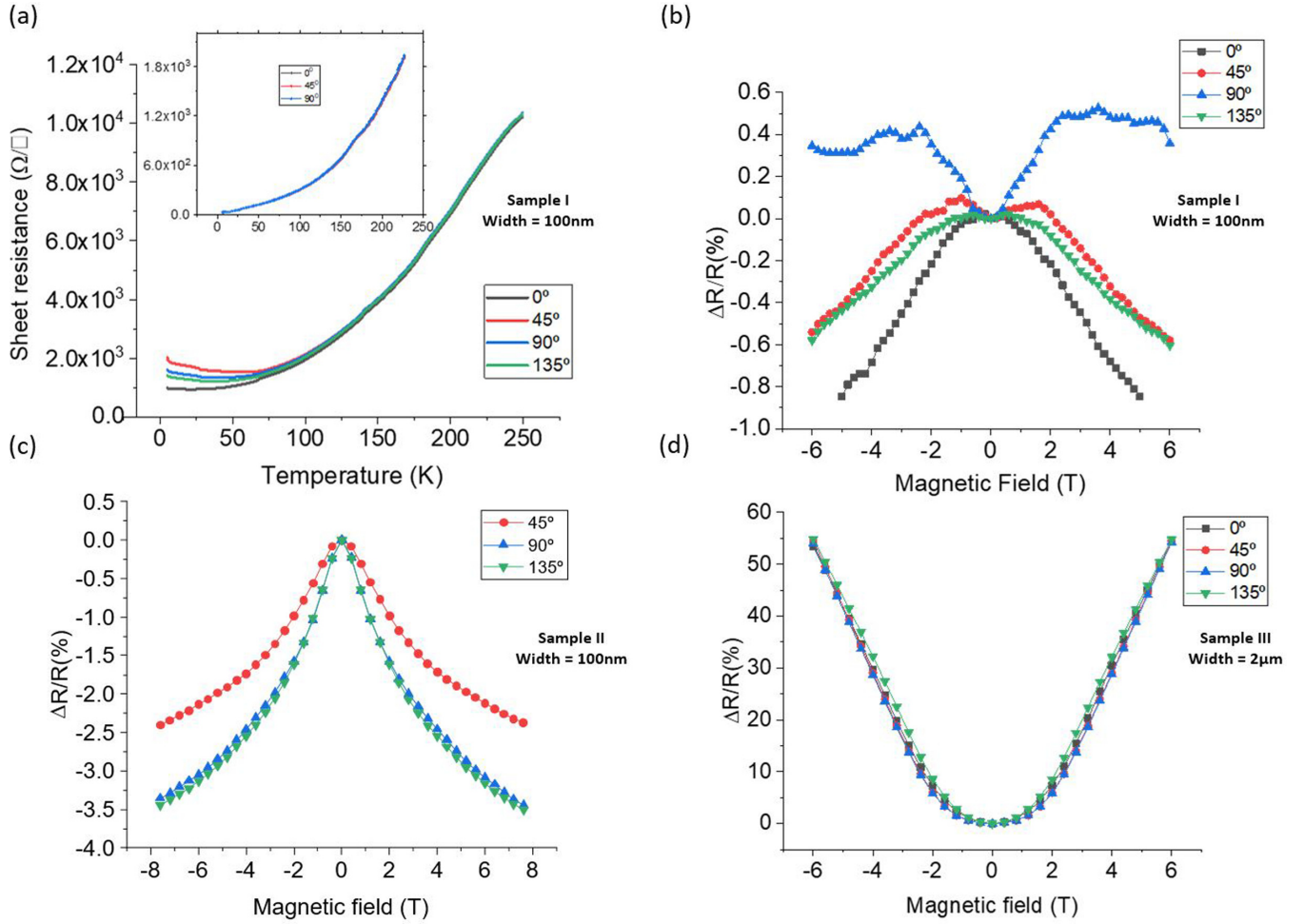


FIG. 2. (a) variation of resistance with temperature for different orientations of a 100 nm wide structure (sample 1). A clear deviation of the resistance for differently aligned sections of the Hall bar appears when the temperature is below 100 K. The inset shows the temperature dependence for a large-area structure. Anisotropy of magnetoresistance with orientation in 100 nm structures from (b) sample 1 and (c) sample 2 and (d) for a 2  $\mu\text{m}$  wide hall bar. For the nanostructures the MR is small compared to the 2  $\mu\text{m}$  structure; however, the anisotropy that is predominant in the nanostructures almost vanishes in the larger Hall bar.

At room temperature there is no significant difference in resistance between the four different orientations of the nanostructures. Also, during cooldown the temperature decreases monotonically and identically for all four structures as expected, but only down to the approximate  $T_{PT}$  of STO (105 K). Below this temperature the four respective resistance values start to deviate. For three of the crystalline directions the resistance also starts to increase again below approximately 40 K, an effect that is not unknown for large-area structures. This increase at lower temperatures is often attributed to the onset of weak localization, electron-electron interaction, or the Kondo effect [5,22,23]. Cooling curves for a set of differently oriented structures of 2  $\mu\text{m}$  width do not show any anisotropy. After this first confirmation we test whether warming and cooling again through  $T_{PT}$  changes the result of the experiment. For the sake of simplicity we measure only the resistance at 4 K. After the initial cooldown the respective sheet resistance values for the four different orientations were 1 k $\Omega/\square$  (0°), 2.1 k $\Omega/\square$  (45°), 1.6 k $\Omega/\square$  (90°), and 1.4 k $\Omega/\square$  (135°). This difference in sheet resistance values along different stripes is in agreement with

random orientation of domain walls and filamentary conduction. We observed no significant change in sheet resistance when the sample was heated to  $T_{\text{max}} < T_{PT}$ . For heating with  $T_{\text{max}} > T_{PT}$  the sheet resistances change significantly but still randomly to 2 k $\Omega/\square$  (0°), 2.2 k $\Omega/\square$  (45°), 2.7 k $\Omega/\square$  (90°), and 1.7 k $\Omega/\square$  (135°). This is consistent with the random formation of domain walls at  $T_{PT}$ . We have repeated the experiment several times and also for different structures. Although we might have expected a preference for higher or lower resistance values for certain crystalline orientations, we cannot observe any significant preference for higher or lower values for any crystalline direction. The reason could be too low a number of experiments for valid statistics or the absence or smallness of the effect.

Our next goal was to investigate the magnetoresistance (MR) in differently oriented nanostructures. For the MR measurements the magnetic field was applied perpendicular to the sample surface. The field was swept from  $B = -6$  T to  $B = +6$  T. We first discuss the magnetoresistance for structures of 2  $\mu\text{m}$  width. Independent of the orientation, these structures show a large positive magnetoresistance which is

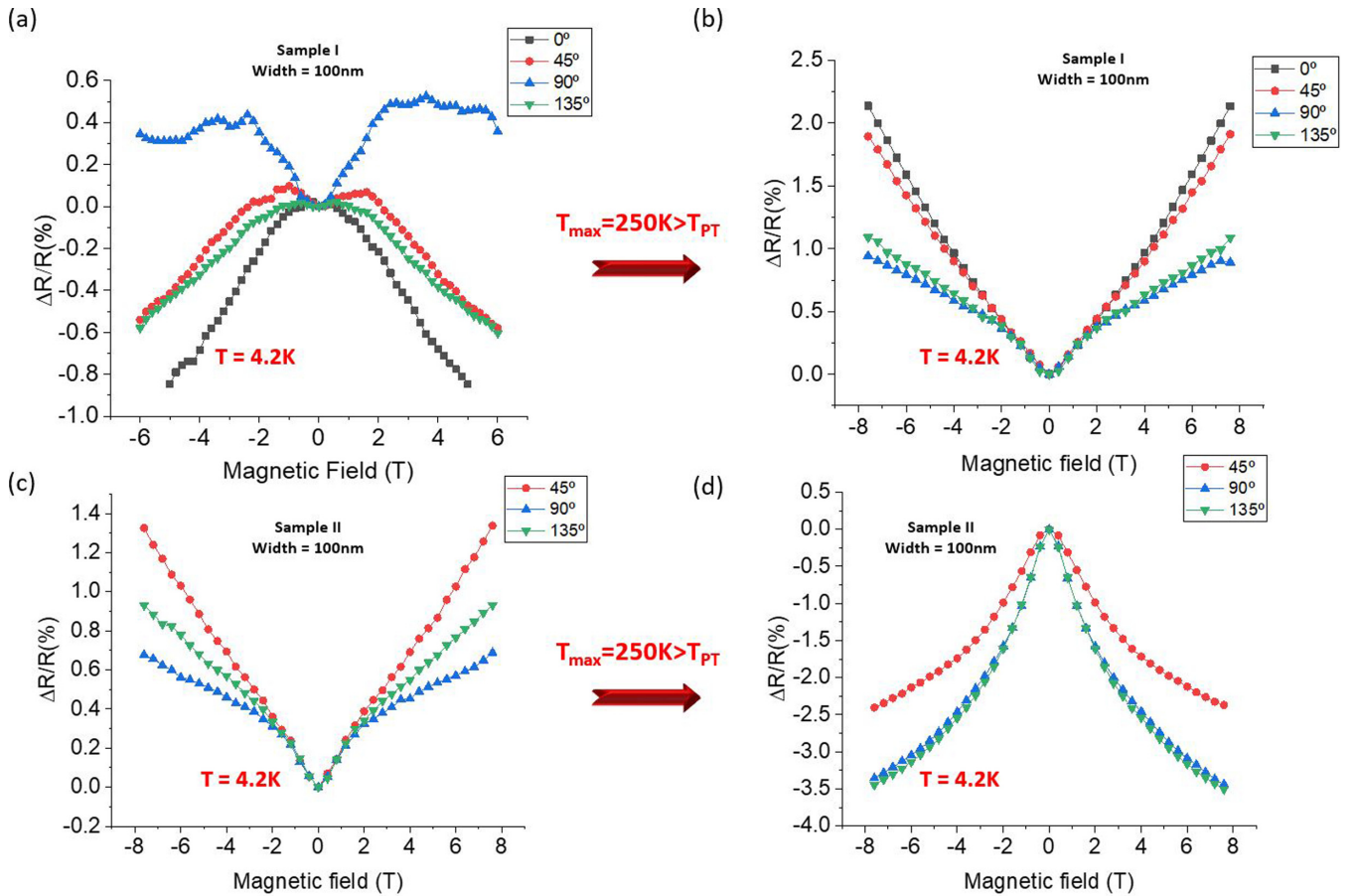


FIG. 3. Variation of MR at  $T = 4.2$  K for two different samples when a warm-up-cooldown cycle is performed to  $250\text{ K} > T_{PT}$ . Both samples are heated to  $250\text{ K} > T_{PT}$  and then held for 1 h and finally cooled down to  $4.2\text{ K}$ , and then the measurement was done at  $4.2\text{ K}$ . Both (a) and (b) sample 1 and (c) and (d) sample 2 show significant change in MR behavior after the warmup through  $T_{PT}$ . Not only the magnitude but also the sign of the MR changes.

quadratic in magnetic field, as shown in Fig. 2(d). This out-of-plane positive MR is due to orbital effects often dubbed ordinary magnetoresistance [22,24–26]. This quadratic MR is in good agreement with existing multiband models for large-area LAO/STO because it can appear only when more than one band contributes to the transport cite [27–29]

It should be noted that there are small differences in the MR for differently oriented stripes; nevertheless, the main contribution is identical for all orientations. For nanostructures we get a completely different picture. Figures 2(b) and 2(c) show two sets of MR curves taken on two different samples. The curves in each diagram were taken simultaneously for different parts of a single Hall bar with different respective crystalline orientations. We immediately notice that the relative MR of the structures is much smaller than for the larger structure. The large ordinary positive MR observed in the  $2\text{ }\mu\text{m}$  wide bars that showed a relative MR of  $\Delta R/R > 50\%$  at  $B = 6\text{ T}$  [Fig. 2(d)] has completely vanished. The MR in the nanostructures is smaller than 1% for the first structure and a few percent for the other one. Furthermore, the sign and/or magnitude of the MR differ for all orientations. The similarity of the curves for  $45^\circ$  and  $135^\circ$  for the first structure is purely random and cannot be reproduced in other samples. The fact that the magnitude of the MR in a large-area structure in Fig. 2(d) is at least one order of magnitude higher than for

the nanostructures indicates that the physics associated with the origin of MR can be different, as will be discussed below.

In a next step we investigate the MR after warm-up and cooldown through  $T_{PT}$ . Both structures were warmed up to  $250\text{ K}$  and cooled down again to  $4.2\text{ K}$ . Figure 3 shows the results for structures 1 and 2, respectively. In both cases the MR has changed considerably. Especially for structure 2, we observe a change in magnitude and sign for all three measured directions. Further temperature sweeps show that the phase transition seems to be crucial for the effect. Figure 4 shows a further sequence of MR measurements after different warm-up and cooling cycles for structure 2. After the measurement from Fig. 3 the sample was first warmed up to  $75\text{ K}$ , which is below  $T_{PT}$ . The sample was kept at this temperature for 60 min and then cooled down to  $4.2\text{ K}$  again. The resulting MR measurements look identical [Fig. 4(b)] to the previous ones. The sample is then warmed up to  $220\text{ K}$ , which is above  $T_{PT}$ . After again cooling the sample down to  $4.2\text{ K}$ , we observe a moderate change in the magnitude of the MR, especially for an angle of  $90^\circ$  [Fig. 4(c)]. Repeating the same sequence warming up to  $75\text{ K}$  for 1 h and cooling down yields no change [Fig. 4(d)]. Warming up again through  $T_{PT}$  ( $T_{\max} = 220\text{ K}$ ) for 1 h, however, results in a massive change [Fig. 4(e)]. For  $90^\circ$  and  $135^\circ$  the MR is reduced by a factor of  $\approx 7$ . For the  $45^\circ$  direction, however, we observe a complete sign reversal of the MR.

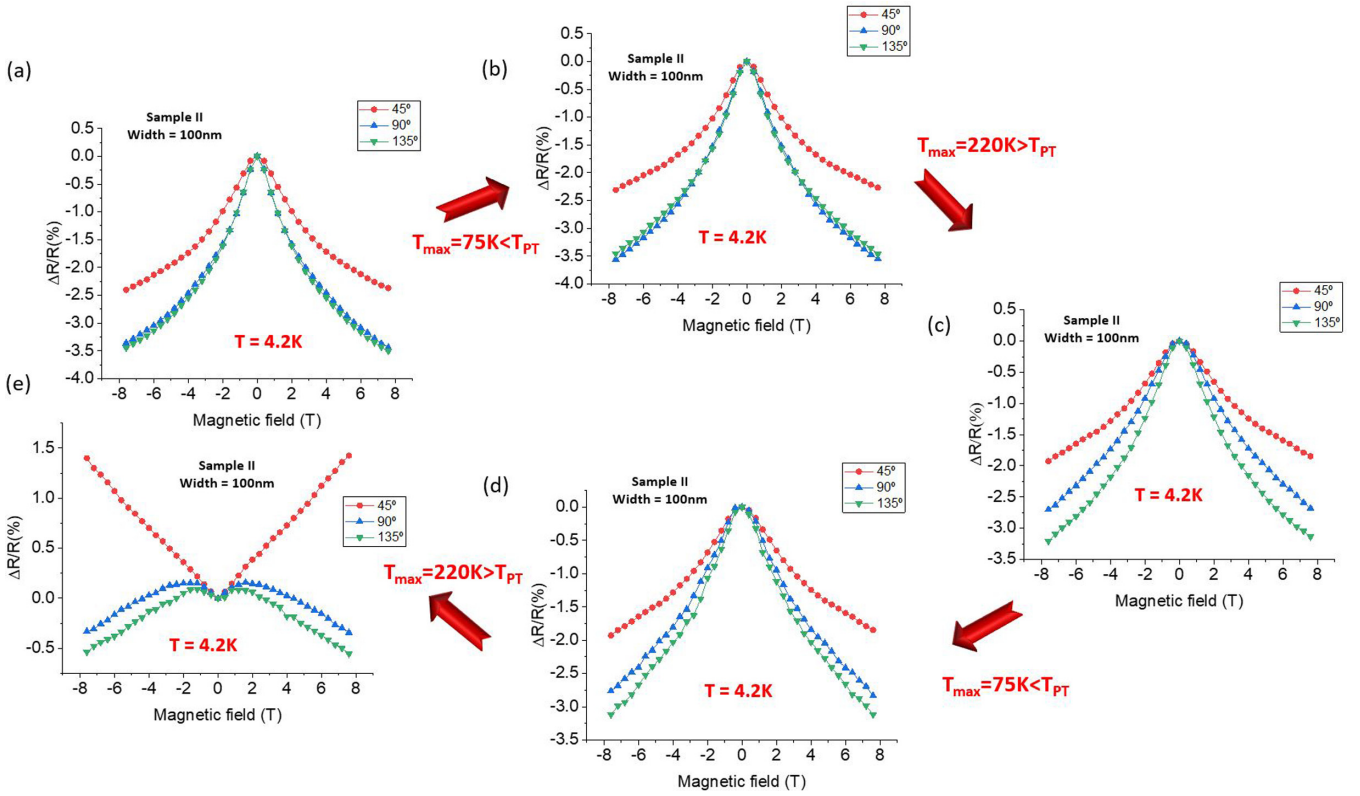


FIG. 4. Magnetoresistance curves for 100 nm wide segments of an LAO/STO Hall bar at  $T = 4.2$  K after various temperature cycles. (a) After the first cooldown all segments show only negative MR, possibly related to weak localization. (b) After cycling to  $T = 75$  K ( $< T_{PT}$ ) and back, no change is observed. (c) After warming up to  $T = 220$  K ( $> T_{PT}$ ), which is well above  $T_{PT} = 105$  K, a small modification is observed; however, all MR curves are still negative. (d) Cycling to 75 K again yields no change. (e) A second cycle through the  $T_{PT}$  finally results in a massively modified picture in which one of the curves shows only positive MR, while the other two exhibit a crossover from positive MR at low fields to negative MR at high fields.

As pointed out by Minhas *et al.* [13] the effect of the domain walls is very pronounced for structures as small as 100 nm, but it averages out when the lateral size of the structures is even moderately increased to a few hundred nanometers. The investigation of further samples with lateral dimensions of 200 and 300 nm confirms this statement.

In Fig. 5 we show the MR for 200 and 300 nm wide nanostructures and the change in MR when heating through  $T_{PT}$ . For the 200 nm structure [Figs. 5(a) and 5(b)], the MR obtained is hugely direction dependent and has lower magnitude, just like in the case of the 100 nm structure. After cycling the temperature through  $T_{PT}$  a significant change is observed. For a 300 nm wide structure [Figs. 5(c) and 5(d)], however, the MR is larger in magnitude and quadratic in nature, as was the case for the 2  $\mu$ m structure [Fig. 2(d)], apparently recovering the contribution of the ordinary magnetoresistance. After sweeping the sample temperature through  $T_{PT}$ , the main quadratic behavior remains unchanged, and only small changes in magnitude appear, as we might expect for a sample that is still close to the critical size.

#### IV. DISCUSSION

We now discuss these results with respect to the initial assumptions:

(1) As expected for conduction through interconnected domain walls, we observe the random scattering of resistance values not only for differently oriented segments of a Hall bar. Even for a single segment cycling the temperature through  $T_{PT}$  leads to a change in low-temperature resistance. The different possible domain wall configurations may also be the cause of the nonmonotonicity of the resistance-temperature curve that sometimes is observed and sometimes is not. It is easily understood that depending on the domain wall properties and the changing dielectric constant at low temperature, rearrangement of the carrier distribution can lead to a change in resistance that can be either positive or negative.

(2) A correlation between crystalline directions and resistance cannot be confirmed. However, it must be stated that due to the randomness of the domain wall distributions statistics on a much larger number of experiments would be necessary to either confirm or dismiss the assumption.

(3) For the magnetoresistance the results are more complex. For structures that are 200 nm wide or smaller we distinguish three different types of MR. In some curves [Figs. 3(b) and 3(c)] we observe only a positive MR. Many curves show only a negative magnetoresistance, but in some cases we also observe a crossover between the two shapes similar to that seen by [24] in LAO/STO with high carrier density or in other 2D disordered metals [30,31]. None of

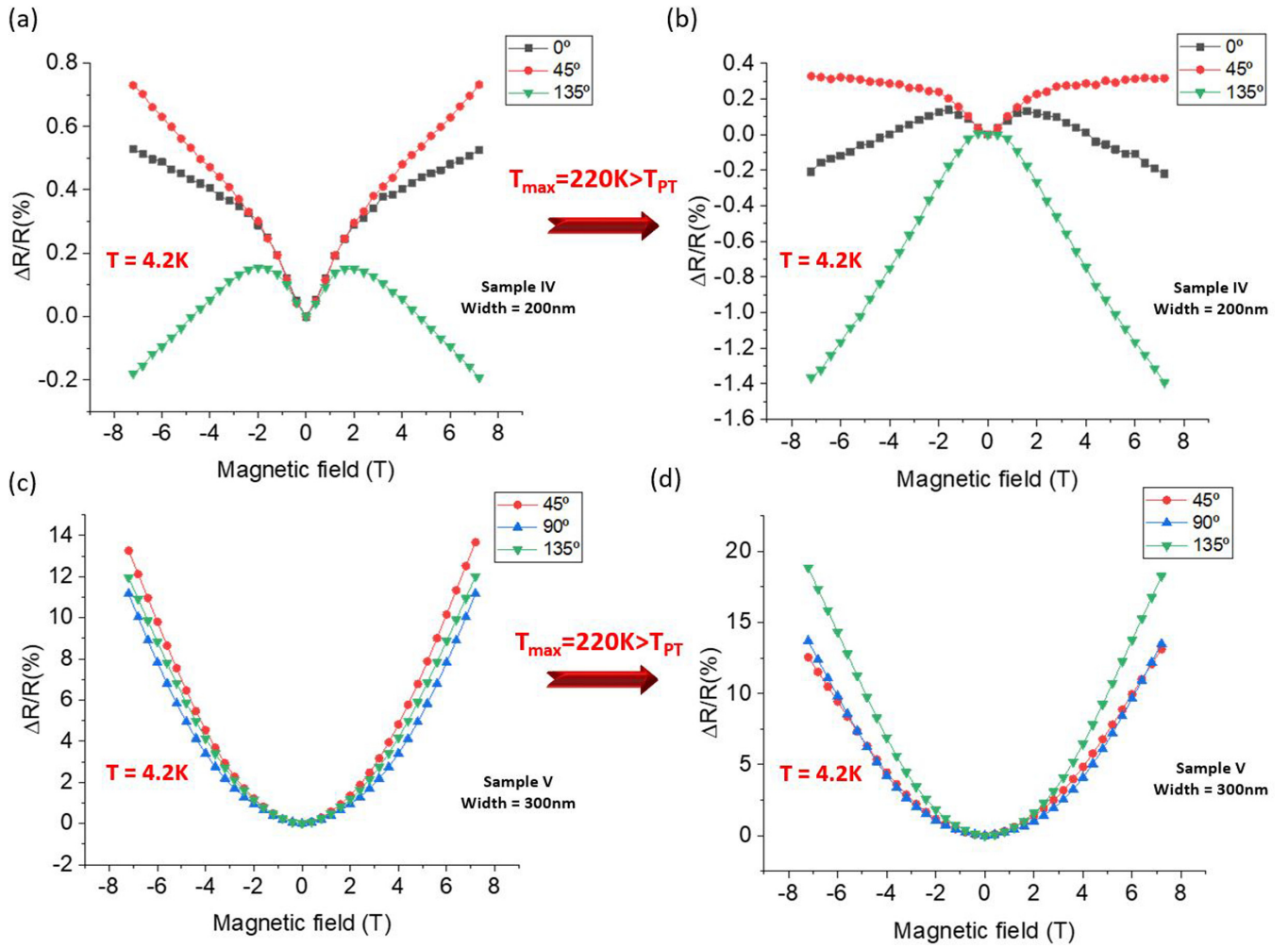


FIG. 5. Magnetoresistance curves for 200 and 300 nm wide segments of an LAO/STO Hall bar at  $T = 4.2 \text{ K}$ . (a) For the 200 nm wide structure the first cooldown results in a small positive magnetoresistance for two segments, while the third segment shows a crossover from positive MR at low magnetic fields to negative MR at high fields. (b) Cycling the temperature through  $T_{PT}$  changes the MR in all three segments. (c) For a 300 nm wide Hall bar, the MR for all segments is dominated by a large quadratic ordinary MR. (d) After cycling the temperature through  $T_{PT}$  this contribution remains dominant, although small differences in the slope appear that may be due to other contributions that are still slightly visible.

the curves, however, shows a clear positive parabolic MR that would indicate dominating ordinary MR. Within our statistics the type of curve does not depend on the crystalline orientation of the investigated segment, and a warm-up-cooldown cycle through  $T_{PT}$  can change the MR from one type to another. In the following we will discuss the underlying physics.

It is well known that in a 2D or quasi-2D system like the domain walls the orientation of the magnetic field with respect to the plane is crucial for the magnetoresistance. For magnetic fields perpendicular to an unpatterned LAO/STO interface the magnetoresistance is often dominated by the positive ordinary magnetoresistance contribution [22,24–26], which is attributed to orbital effects. As mentioned above, this contribution has a quadratic field dependence. Ordinary magnetoresistance is effectively suppressed if either the magnetic field is applied in plane or the dimensions of the structure are too small to allow for orbital effects. Because the type 1 and type 2 domain walls are either perpendicular to or tilted with respect to the surface, a field applied perpendicular to the

interface and thus to the surface can never be perpendicular to either of these domain walls. In addition the extent of the conducting domain walls into the STO is small, efficiently suppressing ordinary MR even for domain walls tilted with respect to the field. Without the ordinary magnetoresistance to compete with, other contributions can start to dominate. A small but purely negative MR [Figs. 4(a)–4(d)] at low temperatures can be caused by weak localization (WL) [32]. A purely positive MR can be due to electron-electron interaction [22,26,33,34] or weak antilocalization (WAL) [35]. The latter requires a significant spin-orbit coupling which, at first glance, is unexpected in STO, which is composed of lighter elements. However, the domain walls at low temperatures are subject to large electric fields that may cause the WAL. Finally, a transition from positive to negative magnetoresistance in a single curve [Figs. 4(e), 5(a), and 5(b)] is explained by a crossover between WAL and WL [24,30,31].

Unfortunately, it is not possible to design a simple model that describes quantitatively the resistance values based on

two types of domain walls with fixed resistivity. Among other aspects the conductivity of the domain walls is determined by the respective number of carriers in the domain wall. Assuming that the initial number of carriers is constant, different domain wall configurations with different total lengths and different contributions from type 1 and type 2 must have different conductivities and will thus contribute differently to the MR. It is even unclear whether the carrier concentration is homogeneous through the domain walls or can vary between different positions.

## V. CONCLUSION

In conclusion we state that in our experiments we found effects that can be predicted based on the theory of filamentary

transport but that do not fit the model of a quasi-2D electron gas with sheet conductivity at the LAO/STO interface. Both resistance and magnetoresistance have random values within a certain range consistent with the formation of two different types of conducting domain walls with different orientation with respect to the surface. The results point out the fact that in the case of small-area structures the microscopic domain wall structure needs to be taken into account to explain various transport phenomena which may not necessarily be explained by the existing theories for large-area structures.

## ACKNOWLEDGMENTS

We wish to acknowledge the support of the Deutsche Forschungsgemeinschaft in SFB762, Project No. B09.

- 
- [1] J. Mannhart and D. G. Schlom, *Science* **327**, 1607 (2010).
- [2] A. Ohtomo and H. Hwang, *Nature (London)* **427**, 423 (2004).
- [3] N. Reyren, S. Thiel, A. D. Caviglia, L. F. Kourkoutis, G. Hammerl, C. Richter, C. W. Schneider, T. Kopp, A.-S. Retschi, D. Jaccard, M. Gabay, D. A. Muller, J.-M. Triscone, and J. Mannhart, *Science* **317**, 1196 (2007).
- [4] S. Thiel, G. Hammerl, A. Schmehl, C. W. Schneider, and J. Mannhart, *Science* **313**, 1942 (2006).
- [5] A. Brinkman, M. Huijben, M. Van Zalk, J. Huijben, U. Zeitler, J. Maan, W. G. van der Wiel, G. Rijnders, D. H. Blank, and H. Hilgenkamp, *Nat. Mater.* **6**, 493 (2007).
- [6] E. Lesne, Y. Fu, S. Oyarzun, J. Rojas-Sánchez, D. C. Vaz, H. Naganuma, G. Sicoli, J. Attané, M. Jamet, E. Jacquet, J.-M. George, A. Barthélémy, H. Jaffrès, A. Fert, M. Bibes, and L. Vila, *Nat. Mater.* **15**, 1261 (2016).
- [7] P. Irvin, J. P. Veazey, G. Cheng, S. Lu, C.-W. Bark, S. Ryu, C.-B. Eom, and J. Levy, *Nano Lett.* **13**, 364 (2013).
- [8] A. Dubroka, M. Rössle, K. W. Kim, V. K. Malik, L. Schultz, S. Thiel, C. W. Schneider, J. Mannhart, G. Herranz, O. Copie, M. Bibes, A. Barthélémy, and C. Bernhard, *Phys. Rev. Lett.* **104**, 156807 (2010).
- [9] S. Meaney, A. Pan, A. Jones, and S. Fedoseev, *APL Mater.* **7**, 101105 (2019).
- [10] F. Schoofs, M. Egilmez, T. Fix, J. L. MacManus-Driscoll, and M. G. Blamire, *Appl. Phys. Lett.* **100**, 081601 (2012).
- [11] S. Seri, M. Schultz, and L. Klein, *Phys. Rev. B* **87**, 125110 (2013).
- [12] N. J. Goble, R. Akrobetu, H. Zaid, S. Sucharitakul, M.-H. Berger, A. Schirlioglu, and X. P. Gao, *Sci. Rep.* **7**, 44361 (2017).
- [13] M. Minhas, A. Müller, F. Heyroth, H. H. Blaschek, and G. Schmidt, *Sci. Rep.* **7**, 5215 (2017).
- [14] B. Kalisky, E. M. Spanton, H. Noad, J. R. Kirtley, K. C. Nowack, C. Bell, H. K. Sato, M. Hosoda, Y. Xie, Y. Hikita, C. Woltmann, G. Pfanzelt, R. Jany, C. Richter, H. Y. Hwang, J. Mannhart, and K. A. Moler, *Nat. Mater.* **12**, 1091 (2013).
- [15] F. W. Lytle, *J. Appl. Phys.* **35**, 2212 (1964).
- [16] M. Honig, J. A. Sulpizio, J. Drori, A. Joshua, E. Zeldov, and S. Ilani, *Nat. Mater.* **12**, 1112 (2013).
- [17] Y. Frenkel, N. Haham, Y. Shperber, C. Bell, Y. Xie, Z. Chen, Y. Hikita, H. Y. Hwang, and B. Kalisky, *ACS Appl. Mater. Interfaces* **8**, 12514 (2016).
- [18] H. J. Harsan Ma, S. Scharinger, S. W. Zeng, D. Kohlberger, M. Lange, A. Stöhr, X. R. Wang, T. Venkatesan, R. Kleiner, J. F. Scott, J. M. D. Coey, D. Koelle, and Ariando, *Phys. Rev. Lett.* **116**, 257601 (2016).
- [19] P. Krantz and V. Chandrasekhar, *Phys. Rev. Lett.* **127**, 036801 (2021).
- [20] M. Minhas, H. Blaschek, F. Heyroth, and G. Schmidt, *AIP Adv.* **6**, 035002 (2016).
- [21] T. Hupfauer, A. Matos-Abiague, M. Gmitra, F. Schiller, J. Loher, D. Bougeard, C. H. Back, J. Fabian, and D. Weiss, *Nat. Commun.* **6**, 7374 (2015).
- [22] D. Fuchs, A. Sleem, R. Schäfer, A. G. Zaitsev, M. Meffert, D. Gerthsen, R. Schneider, and H. v. Löhneysen, *Phys. Rev. B* **92**, 155313 (2015).
- [23] T. Schneider, A. D. Caviglia, S. Gariglio, N. Reyren, and J.-M. Triscone, *Phys. Rev. B* **79**, 184502 (2009).
- [24] F. J. Wong, R. V. Chopdekar, and Y. Suzuki, *Phys. Rev. B* **82**, 165413 (2010).
- [25] M. Ben Shalom, C. W. Tai, Y. Lereah, M. Sachs, E. Levy, D. Rakhmilevitch, A. Palevski, and Y. Dagan, *Phys. Rev. B* **80**, 140403(R) (2009).
- [26] H. Xue, C. Li, Y. Hong, X. Wang, Y. Li, K. Liu, W. Jiang, M. Liu, L. He, R. Dou, C. Xiong, and J. Nie, *Phys. Rev. B* **96**, 235310 (2017).
- [27] S. Lerer, M. Ben Shalom, G. Deutscher, and Y. Dagan, *Phys. Rev. B* **84**, 075423 (2011).
- [28] M. Ben Shalom, A. Ron, A. Palevski, and Y. Dagan, *Phys. Rev. Lett.* **105**, 206401 (2010).
- [29] P. Seiler, J. Zabaleta, R. Wanke, J. Mannhart, T. Kopp, and D. Braak, *Phys. Rev. B* **97**, 075136 (2018).
- [30] Y. F. Komnik, V. Andrievskii, and I. Berkutov, *Low Temp. Phys.* **33**, 79 (2007).
- [31] T. Kawaguti and Y. Fujimori, *J. Phys. Soc. Jpn* **52**, 722 (1983).
- [32] E. Abrahams, P. W. Anderson, D. C. Licciardello, and T. V. Ramakrishnan, *Phys. Rev. Lett.* **42**, 673 (1979).
- [33] S. Das, A. Rastogi, L. Wu, J.-C. Zheng, Z. Hossain, Y. Zhu, and R. C. Budhani, *Phys. Rev. B* **90**, 081107(R) (2014).
- [34] P. Kumar, A. Dogra, P. Bhadauria, A. Gupta, K. Maurya, and R. Budhani, *J. Phys.: Condens. Matter* **27**, 125007 (2015).
- [35] A. D. Caviglia, M. Gabay, S. Gariglio, N. Reyren, C. Cancellieri, and J.-M. Triscone, *Phys. Rev. Lett.* **104**, 126803 (2010).